

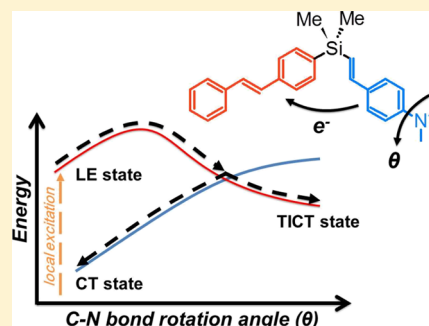
C–N Bond Rotation Controls Photoinduced Electron Transfer in an Aminostyrene–Stilbene Donor–Acceptor System

Yen-Chin Huang and Yuan-Chung Cheng*[✉]

Department of Chemistry, National Taiwan University, No. 1, Sec. 4, Roosevelt Rd., Da-an District, Taipei City 106, Taiwan

Supporting Information

ABSTRACT: We investigate energy transfer and electron transfer in a dimethylsilylene-spaced aminostyrene–stilbene donor–acceptor dimer using time-dependent density functional theory calculations. Our results confirm that the vertical S_3 , S_2 , and S_1 excited states are, respectively, a local excitation on the aminostyrene, local excitation on the stilbene, and the charge-transferred (CT) excited state with electron transfer from aminostyrene to stilbene. In addition, an energy minimum with the C–N bond of the amino group twisted at about 90° is also identified on the S_1 potential energy surface. This S_1 state exhibits a twisted intramolecular charge transfer (TICT) character. A potential energy scan along the C–N bond torsional angle reveals a conical intersection between the S_2 stilbene local excitation and the S_1 CT/TICT state at a torsional angle of $\sim 60^\circ$. We thus propose that the conical intersection dominates the electron transfer dynamics in the donor–acceptor dimer and copolymers alike, and the energy barrier along the C–N bond rotation controls the efficiency of such a process. Moreover, we show that despite the zero oscillator strength of the S_1 excited states in the CT and TICT minima, an emissive S_1 state with a V-shaped conformational structure can be located. The energy of this V-shape CT structure is thermally accessible; therefore, it is expected to be responsible for the CT emission band of the dimer observed in polar solvents. Our data provide a clear explanation of the complex solvent-dependent dual emission and photoinduced electron transfer properties observed experimentally in the dimer and copolymer systems. More importantly, the identifications of the conical intersection and energy barrier along the C–N bond rotation provide a novel synthetic route for controlling emissive properties and electron transfer dynamics in similar systems, which might be useful in the design of novel organic optoelectronic materials.



1. INTRODUCTION

Functional organic materials incorporating both donor and acceptor chromophores in the molecular backbone are fundamental in light emitting, light harvesting, artificial photosynthesis, and sensing applications.^{1,2} In particular, various linear polymers with alternating donor and acceptor moieties connected by silylene spacers have recently drawn considerable research attention because of their applications in light-harvesting materials,^{3–6} electron transfer materials,^{7,8} and polymer foldamers.^{9–11} In these alternating copolymer systems, the silylene bridge acts as an insulating spacer that prevents electronic delocalization between neighboring chromophores, while still allowing efficient through-space energy transfer or charge transfer between the chromophores to occur.^{12–14} This design hence enables a great deal of tunability in the photophysical properties of the materials by controlling the chemical compositions of the individual donor and acceptor segments. On the other hand, complex polymer folding behavior and strongly solvent-dependent photoinduced electron transfer dynamics have also been observed in these silylene-spaced copolymer systems, making the full elucidation of their photophysical behaviors extremely nontrivial.^{6,8–11,15,16}

Among the synthetic silylene-spaced copolymer systems, the dimethylsilylene-spaced aminostyrene–stilbene copolymers

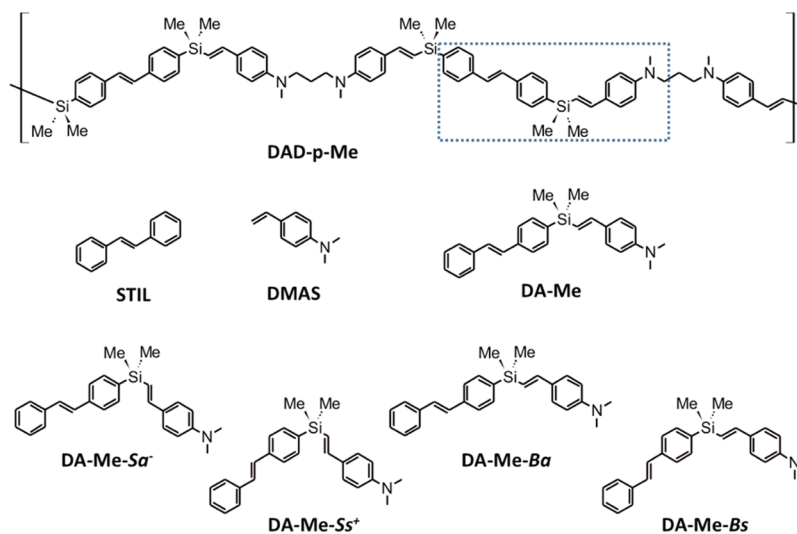
(Scheme 1) might be the one group with unusual photo-physical properties that are the most challenging to fully understand. Photoinduced electron transfer from aminostyrene to stilbene has been observed in oligomers and copolymers; therefore, the aminostyrene–stilbene pair is designated as a donor–acceptor (DA) dimer with aminostyrene as the electron donor and stilbene as the acceptor. Such aminostyrene–stilbene dimer forms the basic subunit of the copolymers (Scheme 1). Steady-state spectra show that the oligomers and copolymers exhibit dual emission from the stilbene local excitation and charge-transfer state, and the emissive properties depend strongly on the solvent polarity and degree of polymerization. As a result, the charge-transfer emission has been adopted as a sensitive probe for the polymer folding in similar alternative copolymer systems. However, the mechanisms of charge transfer and the sensitivity to the solvent polarity have never been clearly elucidated. Recently, time-resolved spectroscopy has observed sub-ps energy transfer, electron transfer, and ~ 10 ps structural relaxation in the aminostyrene–stilbene dimer system. However, the detailed

Received: January 28, 2019

Revised: April 8, 2019

Published: April 29, 2019

Scheme 1. Chemical Structures of the Compounds Studied in This Work



mechanisms and the driving force for the ultrafast electronic transfer processes remain unclear or even controversial. For example, the local excitation band was assigned to aminostyrene emission by Yao et al.,¹⁶ which is contrary to previous assignments and density functional theory (DFT) calculation results.^{8,10} Generally speaking, the mechanisms for the ultrafast photoinduced electron transfer (~ 1 ps), dual emission in medium polar solvents, and low fluorescence quantum yield in the copolymers are yet to be fully investigated.

In this work, we focus on the dimethylsilylene-spaced dimethylaminostyrene–stilbene dimer (**DA-Me**, in Scheme 1), which is the basic unit of the copolymer system. We aim to apply theoretical calculations to explore the detailed excited-state properties of the **DA-Me** system. In contrast to previous theoretical studies that put the focus on the vertical excitation properties and couplings of the molecular chromophores, we will explore the full excited-state potential energy surfaces (PES) of the **DA-Me** dimer system in order to fully elucidate the photophysical dynamics. We propose that this dynamical perspective is crucial in order to reach a general understanding of the complex energy transfer and photoinduced electron transfer dynamics in molecular DA systems, as has been demonstrated in various theoretical studies.^{17–23} Especially, it is well known that the C–N bond rotation in the aminostyrene could lead to a twisted intramolecular charge transfer (TICT) state, and we believe this TICT formation dynamics should not be overlooked. We will pay extra attention to investigate the effects of the C–N bond rotation on the photophysics of **DA-Me**.

2. MODELS AND THEORETICAL CALCULATIONS

Scheme 1 shows the chemical structures of the model systems studied in this work, including the stilbene (**STIL**), dimethylaminostyrene (**DMAS**), and dimethylsilylene-spaced DA dimer (**DA-Me**). We found that the dimer **DA-Me** exhibits 4 conformational energy minima, whose structures and labeling are also shown in Scheme 1 (also see Figure S1). **STIL**, **DMAS**, and **DA-Me** are subunits of the alternative copolymer **DAD-p-Me**, and we carried out theoretical calculations for them as the foundation to elucidate the photoinduced energy transfer and electron transfer processes in the copolymer system.

All quantum chemical calculations were performed using the Gaussian 09 software package.²⁴ DFT and time-dependent DFT (TDDFT) calculations at the B3LYP-D3/6-31+G(d) level were used for obtaining optimized geometries of the ground state (GS) and first three excited states for **STIL**, **DMAS**, and **DA-Me** (Scheme 1) without any symmetry constraint. Vibrational analysis for the optimized geometries in the GS was carried out to ensure the stability of the optimized structures. B3LYP exchange–correlation functional²⁵ was successfully adopted by Hsu and co-workers to calculate equilibrium geometry and excited-state properties of silylene-spaced divinylbiphenyl–divinylstilbene dimers, which are similar to our system,^{14,15} so we are convinced that this level of theory is reliable. Dispersion interaction between aminostyrene moiety and stilbene moiety may play an important role in excited-state properties and relative energy of conformers; hence, Grimme's D3 correlations were used in our calculations.²⁶ We note that the validity of the B3LYP functional in treating charge-transfer states must be carefully examined in order to provide reliable results. To this end, we also carried out calculations using the M062X-D3 functional²⁷ for the **DA-Me** dimer as benchmarks.

We calculate electronic transitions and molecular orbitals based on the optimized structures in the GS as well as optimized geometries of various excited states. To explore the PES along the C–N bond rotation in the excited states, linear synchronous transit method²⁸ was applied. This method uses a simple linear geometric interpolation between two structures to create a path connecting the two structures. To generate the transition route from the Franck–Condon point (the GS optimized geometry) to the S_1 TICT geometry, we first performed a constrained GS geometry optimization at the 90° rotational angle and then used the linear synchronous transit method to generate paths between 0° angle and 45° angle and between 45° angle and 90° angle, respectively. Vertical transitions of each point on the route were calculated using TDDFT/B3LYP-D3/6-31+G(d). Compared to a relaxed scan that could lead to a large geometrical relaxation between two consecutive structure points, the linear synchronous transit method yields structures that are smoothly connected and therefore a better representation of the PES.

3. RESULTS AND DISCUSSION

3.1. Excited-State Properties of the Monomers. Before we present the results for the **DA-Me** dimer system, we first investigate the excited-state properties of the **STIL** and **DMAS** monomers. Table 1 presents excited-state properties of the

Table 1. Calculated Excited-State Properties of the Monomers (STIL and DMAS) at the TDDFT/B3LYP/6-31+G(d) Level of Theory

model	structure ^a	λ (nm)	f_{S_1}	major configuration(s) ^b
STIL	GS	322	0.92	H \rightarrow L (99%)
STIL	ES ₁	373	0.93	H \rightarrow L (98%)
DMAS	GS	305	0.36	H \rightarrow L (82%) H \rightarrow L + 1 (13%)
DMAS	PICT	333	0.34	H \rightarrow L (88%)
DMAS	TICT	445	0.00	H \rightarrow L (98%)

^aGS: ground-state minimum, ES₁: first excited-state minimum.

^bPopulation > 10%.

monomers in the GS as well as the optimized structures in the S₁ excited state (ES₁), whereas the relevant frontier orbitals are presented in Figures S2 and S3. For the S₁ excited state of **STIL**, the theory predicts vertical excitation from the GS minimum at 322 nm and emission from the ES₁ minimum at 373 nm. S₁ is a highest occupied molecular orbital (HOMO) \rightarrow lowest unoccupied molecular orbital (LUMO) $\pi\pi^*$ transition, as expected. For **DMAS**, the vertical transition to S₁ is calculated to be at 305 nm, slightly higher than for the S₁ transition of **STIL**. Geometry optimization at the S₁ PES initialized from the Franck–Condon position (GS minimum) leads to an S₁ energy minimum with a planar structure. The electronic state at this structure corresponds to a HOMO \rightarrow LUMO transition with reduced electron density in the amino group in the LUMO (Figure S3a); thereby, this state is designated as a planar intramolecular charge transfer (PICT) state.

It is well known that the amino-substituted aromatic system could exhibit TICT states through the rotation of the C–N bond.^{1,2} Therefore, we carried out geometry optimization for the S₁ excited state at the C–N bond twisted structure of **DMAS** (Figure S3) and explored the PES of C–N rotation (Figure S4). Indeed, an energy minimum on the S₁ excited state is confirmed at the 90° rotational angle, which corresponds to an $n\pi^*$ transition (TICT state). The vertical transition energy from the **DMAS** TICT state to the GS is calculated as 445 nm (Table 1), which is significantly in lower energy compared to the PICT state. Notably, in the planar geometry, the HOMO and LUMO exhibit significant spatial overlap and the **DMAS** S₁ excitation is delocalized among the whole molecule, leading to the bright PICT excited state. However, the rotation of the C–N bond breaks the conjugation and localizes the excitation. In the twisted TICT geometry, the HOMO–LUMO spatial overlap is negligible (Figure S3b). As a result, the TICT state is a dark state and the PES from the PICT to the TICT state exhibits a small energy barrier of ~ 1 kcal/mol. The small barrier indicates that upon photoexcitation the emissive PICT state should readily convert to the non-emissive TICT state. As a result, the C–N bond twisting plays a significant role in the radiationless decay of the **DMAS** excited states. This might explain the low fluorescence quantum yield of **DMAS**. In addition to its role in the radiationless decay channel, the TICT state and the C–N

bond rotation could play important roles in the photophysics of the dimer and copolymer systems. In this work, we will demonstrate that this is indeed the case. Note that we cannot exclude the existence of additional non-TICT relaxation mechanisms in the **DA-Me** system. The well-studied 4-(*N,N*-dimethylamino)benzotrile (DMABN) system, which shares structural similarities to the **DMAS** system, also exhibits dual emission that is strongly dependent on the solvent properties. Several mechanisms, in addition to the TICT theory, have been proposed to explain the dual emission in the DMABN system and the issue is still debated.^{1,29–32} Nevertheless, the results in this work still support that the C–N bond rotation provides a highly plausible explanation of the full solvent-dependent photophysics of the silylene-spaced DA system.

We summarize our results on the photophysical properties of the monomers in Figure 1. Experiments show that **STIL**

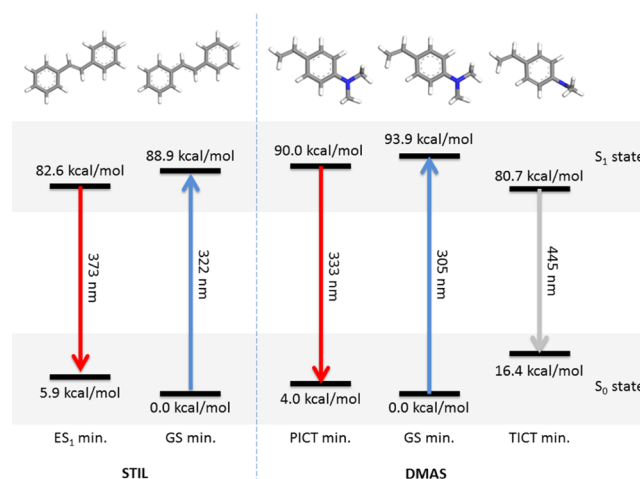


Figure 1. Energy-level diagrams for the **STIL** and **DMAS** monomers.

exhibits an absorption band peaks at 315 nm, whereas **DMAS** shows a broad absorption with a maximum around 305 nm. These values are in excellent agreement with our vertical excitation energy calculations. Furthermore, the experimental emission band maximum of **STIL** and **DMAS** is reported at 365 nm and from 360 to 450 nm, respectively, which is also in good agreement with our calculations.

3.2. Excited States of DA-Me. The dimer **DA-Me** molecule has many conformational states that might have different excited-state properties. To avoid confusion, we first investigate the excited states of **DA-Me-Sa⁻** (Scheme 1). The study of the conformational dependence will be presented later.

We calculated optimized geometry of **DA-Me** and photophysical properties for the three lowest-energy vertical excited states (Table 2). To facilitate the analysis, the frontier molecular orbitals at the GS geometry are presented in Figure 2a. The results show that S₁ is the HOMO \rightarrow LUMO transition, which corresponds to the charge-transferred (CT) transition with electron density shifting from **DMAS** to **STIL**. Because the HOMO and LUMO are separated on different molecules and the π -conjugated systems on the two planar molecules are oriented at a near-orthogonal angle, the HOMO and LUMO exhibit extremely small spatial overlap, leading to negligible transition density for the S₀ \rightarrow S₁ transition. Therefore, the CT state has zero oscillator strength; therefore, it will not be observable in the absorption spectrum. The large

Table 2. Vertical Excitation Properties of the DA-Me-Sa⁻ Dimer (TDDFT/B3LYP/6-31+G(d))

structure ^a	state	λ (nm)	f_{Sn}	major configurations ^b	μ^c	character
GS	S ₀				3.4	
GS	S ₁	399	0.00	H → L (99%)	38.4	CT _{D→A}
GS	S ₂	333	1.26	H - 1 → L (86%) H → L + 1 (13%)	4.3	LE _A
GS	S ₃	312	0.54	H - 1 → L (12%) H → L + 1 (79%)	7.8	LE _D

^aGS: ground-state minimum. ^bPopulation > 10%. ^cUnit: debye.

molecular dipole moment of the S₁ state and the electron density difference map for the S₀ → S₁ transition (Figure S5a) confirm the CT assignment. Furthermore, the S₂ (mainly HOMO - 1 → LUMO) and S₃ (mainly HOMO → LUMO + 1) represent local excitations on the STIL and DMAS, respectively. Our calculation indicates that the two local excitations are slightly (~10%) mixed with each other at the GS optimized structure; therefore, the two chromophores are excitonically coupled, and excitation energy transfer between them should be expected. S₂ and S₃ both have significant oscillator strength, and their transition energies are quite close to each other; therefore, they should both be populated upon photoexcitation. In addition, the electron density difference maps also confirm that the two excited states are mostly localized.

To verify the reliability of the B3LYP method for the dimer CT excitations, we also performed geometry optimization for the DA-Me system using the M06-2X-D3 exchange–correlation functional and calculated the frontier orbitals (Figure S6a). The calculation shows that the HOMO → LUMO transition in the M06-2X-D3 result also corresponds to the CT transition described by electron transfer from DMAS to STIL, consistent with the B3LYP results.

Geometry optimization on the excited-S₂ and S₃ PES results in further localization of the electronic states and energy minimum corresponding to the locally excited (LE) emissive states on the STIL and DMAS moieties, respectively. The vertical emission wavelengths predicted for the relaxed S₂ excited state and the relaxed S₃ excited state are 384 and 332 nm, respectively. Experimental steady-state measurement shows an LE emission centered around 360–370 nm with

weak solvent dependence.¹⁶ The most reasonable assignment of this observed LE emission based on our calculations is from the S₂ local excitation on the STIL moiety. Our calculations show that S₂ has the least charge-transfer character (Figure S5b) and its molecular dipole moment is small, which explains the weak solvent-polarity dependence of the LE emission.

3.3. CT Excitations of DA-Me and Rotation of the C–N Bond. To investigate the CT character of the S₁ excited state of DA-Me, we carried out geometry optimization on the excited-S₁ PES. Two distinctive S₁ minimum energy structures were obtained, and their properties are reported in Table 3. The CT minimum is obtained from geometry optimization near the Franck–Condon geometry, and it represents the relaxed structure of the donor-to-acceptor CT state. On the other hand, when the C–N bond in the dimethylaminostyrene moiety is twisted to near 90°, a new energy minimum on the excited-S₁ PES is discovered. The frontier molecular orbitals of this structure are presented in Figure 2b, and it is clear that the molecular orbital patterns are significantly different from those of the GS structure. The S₁ state at this twisted geometry corresponds to a TICT excitation localized on DMAS. Therefore, we assign this structure to the TICT state. Low-lying electronic excitations at this structure exhibit various charge-transfer characters (Table 3).

We also performed additional M06-2X-D3 calculation to verify the validity of the B3LYP method in predicting the TICT state for the DA-Me system. Geometry optimization using the M06-2X-D3 functional on the S₁ PES using a C–N twisted initial condition leads to a stable TICT geometry, in agreement with the B3LYP results. M06-2X-D3 frontier orbitals at this TICT geometry also confirm that its HOMO → LUMO transition is the DMAS TICT excited state (Figure S6b). Overall, the data shown in Figure S6 suggest that the M06-2X-D3 functional should yield energy curves that are qualitatively similar to the B3LYP results. We believe that a full benchmark on the performance of different exchange–correlation functionals, including more recent range-separated functionals, is out of the scope of the current work. Therefore, in this paper we focus on the discussions of the B3LYP results.

It is important to emphasize that our calculations reveal two energy minima on the S₁ excited state of DA-Me, and the two minima are connected by the C–N bond rotation coordinate. Near the Franck–Condon geometry, the S₁ state is delocalized

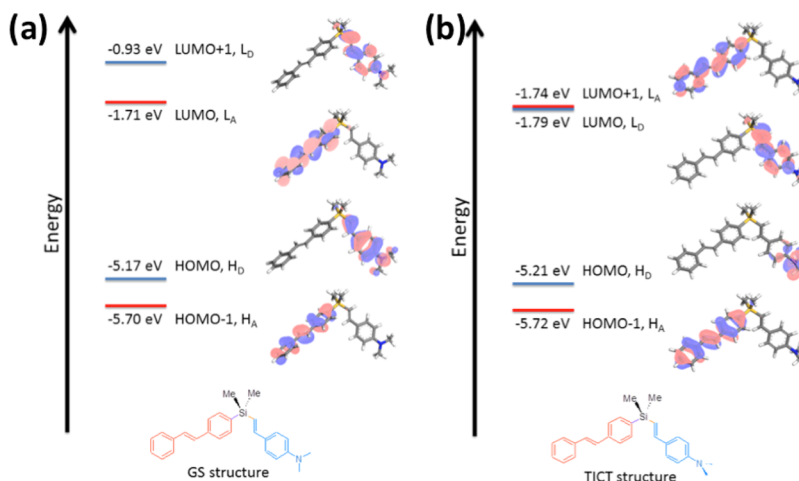
**Figure 2.** Frontier molecular orbitals of DA-Me-Sa⁻ in (a) GS geometry and (b) TICT geometry.

Table 3. Calculated Excited-State Properties of the DA-Me-Sa⁻ Dimer at the CT and TICT Geometries (TDDFT/B3LYP/6-31+G(d))

structure ^a	state	λ (nm)	f_{Sn}	major configurations ^b	μ^c	character
CT	S ₀				3.4	
CT	S ₁	537	0.00	H → L (100%)	33.6	CT _{D→A}
CT	S ₂	370	1.23	H - 1 → L (95%)	3.7	LE _A
CT	S ₃	321	0.61	H → L + 1 (86%)	7.2	LE _D
TICT	S ₀				1.4	
TICT	S ₁	472	0.00	H → L (97%)	16.9	LE _D (TICT)
TICT	S ₂	385	0.00	H → L + 1 (99%)	47.6	CT _{D→A}
TICT	S ₃	352	0.01	H - 1 → L (99%)	30.1	CT _{A→D}
TICT	S ₄	333	1.25	H - 1 → L + 1 (93%)	2.3	LE _A

^aCT: CT minimum, TICT: TICT minimum. ^bPopulation > 10%. ^cUnit: debye.

on both **STIL** and **DMAS**, and it represents an electron-transfer state from **STIL** to **DMAS**. Twisting the C–N bond breaks the π -conjugation on the **DMAS** moiety, causing the excitation to become localized on **DMAS**. As a result, at the near-90° twisting angle, the S₁ state is a TICT state localized on **DMAS**. Hereafter, we use “CT state” to denote the planar delocalized S₁ state and “TICT state” to denote the twisted S₁ state localized on **DMAS**.

To further explore the relationship between the CT state and the TICT state, we apply the linear synchronous transit method²⁷ to map out the PES from the Franck–Condon geometry to the TICT geometry on the S₁ excited state for **DA-Me-Sa⁻**. The obtained adiabatic potential energy curves along the C–N torsional angle are presented in **Figure 3**. The

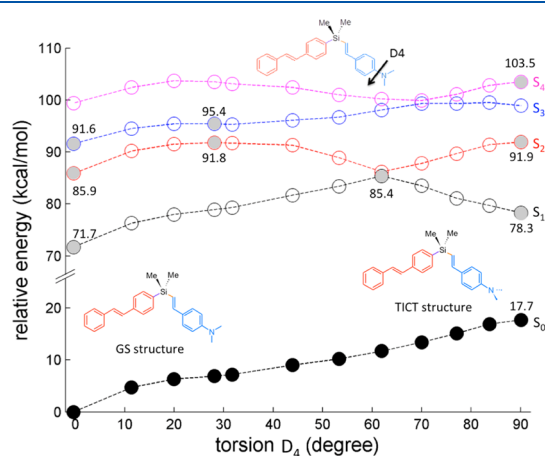


Figure 3. Potential energy curves of S₀–S₄ states as a function of the torsional angle D₄ from the Franck–Condon geometry to the TICT geometry for **DA-Me-Sa⁻**. The gray-filled circles indicate interesting points whose relative energies are labeled on the figure.

results show that the low-lying excited states in the **DA-Me** system undergo several curve crossings upon C–N bond rotation. Most noticeably, the S₁ and S₂ states exhibit a conical intersection at a C–N torsional angle of ~60°. This conical intersection should facilitate rapid S₁ → S₂ nonadiabatic transition, which corresponds to intermolecular electron transfer from **DMAS** to **STIL** (back to CT state) or intramolecular electron transfer within the **DMAS** moiety (proceed to TICT state). In other words, our calculations show that the C–N bond rotation promotes ultrafast S₂ → S₁ nonadiabatic transition in the **DA-Me** dimer, and the transition corresponds to a charge-transfer process in the system. The S₂

→ S₁ nonadiabatic transition could lead to two distinct CT states: one near the planar **DMAS** geometry (CT state) and the other near the twisted **DMAS** geometry (TICT state). Nevertheless, a significant energy barrier of ~6 kcal/mol between the Franck–Condon geometry and the conical intersection should strongly hamper the charge-transfer process in **DA-Me**. Note that our calculations are performed without the inclusion of the solvation effects; therefore, the energy values are only representative of the system in nonpolar solvents. In polar solvents, the energies of both the CT and TICT states should be strongly stabilized. Because the electronic state near the crossing point should exhibit strong mixing between the LE state and the CT state, the energy of the crossing point should decrease as the solvent polarity increases, whereas the energy of the LE state minimum near the Franck–Condon point should remain solvent independent. The electronic state at the energy maximum, thus, has a stronger CT character than the state at the Franck–Condon point. As a result, the energy barrier to the conical intersection is expected to be significantly reduced in polar solvents. We expect this factor to play an important role in the solvent dependence of CT dynamics of the **DA-Me** dimer and copolymer systems, which will be discussed later.

3.4. Conformational Changes and Emissive CT State.

Both the CT state and the TICT state on the S₁ are dark states with zero oscillator strength, which represents a problem in explaining the CT emission observed experimentally in polar solvents. To elucidate this issue, we investigate conformational changes of the **DA-Me** system and search for bright CT states at different conformational structures. DFT calculations indicate that the internal rotations within the **STIL** and **DMAS** molecules exhibit relatively large barriers (**Figures S7 and S8**); therefore, it is reasonable to consider the two subunits as rigid moieties. Therefore, the conformational changes of **DA-Me** mainly depend on two torsional angles: the dihedral angle D₅ between the **STIL** and silylene group, and D₆ between the **DMAS** and silylene group (**Figures 4a and S8**). The D₅ and D₆ Si–C bond rotations lead to four major stable conformational minima (**Scheme 1 and Figure S1**). So far we have presented results based on the **DA-Me-Sa⁻** conformer. TDDFT calculations for the other three conformers were performed and the results are presented in **Tables S1–S3**. We found the vertical excitation properties and the emission properties of these conformers to be quantitatively the same as of the **DA-Me-Sa⁻** conformer.

To obtain the PES for conformational changes of **DA-Me** on the GS and first excited state, we chose optimized conformer **DA-Me-Ba** as the reference geometry and varied the D₅ and

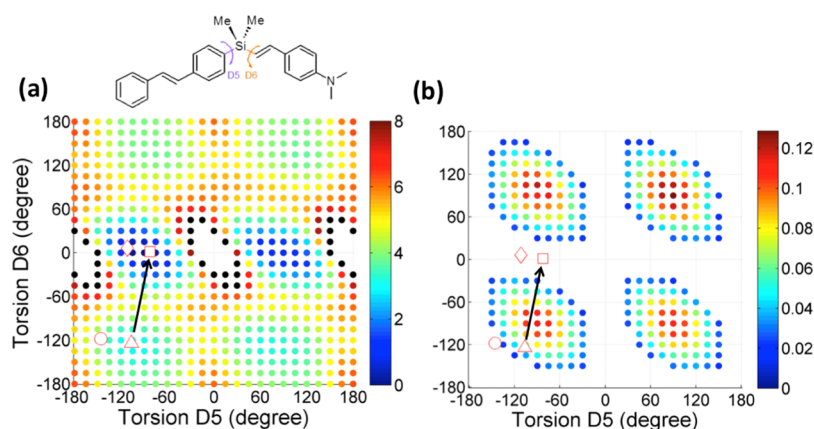


Figure 4. Excited-state properties of DA-Me as functions of the C–Si torsional angles. (a) S_1 PES for the conformational changes of the DA-Me system. Energy is in unit of kcal/mol. The black dots and blank areas represent regions with energy between 8–15 and >15 kcal/mol, respectively. (b) Calculated S_0 – S_1 oscillator strength (f_{S_1}) for the conformational changes of the DA-Me system. \circ and \diamond depict the positions of Franck–Condon geometries for conformers DA-Me-Ba and DA-Me-Sa[−], respectively. \triangle and \square depict the positions of CT geometries for DA-Me-Ba and DA-Me-Sa[−], respectively.

D6 torsional angles to calculate energies using TDDFT. For simplicity, we perform a rigid scan. At each point, only D5 and D6 were varied, whereas other degrees of freedoms were kept frozen. Figure S8 presents the PES for conformational changes in the GS. The results show significant hindered rotation because of the different local geometries of the two groups. The D5 rotation is possible only at $\pm 120^\circ$ D6 angle, whereas the D6 rotation is strongly correlated with the simultaneous rotation of the D6 angle. The energy barrier of D5 and D6 rotations is ~ 2 kcal/mol, suggesting that all the conformers are freely exchangeable at room temperature.

Figure 4a shows the PES for conformational changes in the S_1 excited state. For reference, the Franck–Condon and minimal energy positions of the DA-Me-Sa[−] and DA-Me-Ba conformers are also depicted on the PES map. Rotation of the STIL moiety (dihedral angle D5) from the DA-Me-Ba conformer to the DA-Me-Sa[−] conformer has a very small barrier (indicated by the black arrow), and the conformational change would go through the V-shaped emissive geometry (Figure 4b). Therefore, we expect the two conformers to reach an equilibrium in the excited state if the lifetime is long enough. Such conformational dynamics in the excited state can explain the broad, feature-less absorption and emission bands of the CT state.

To investigate the emissive properties of these conformational structures, we also calculated and mapped out the oscillator strength of the S_1 excited state for the D5 and D6 conformational changes (Figure 4b) for the CT state. Interestingly, a large number of conformational structures with significant oscillator strength ($f > 0.1$) exist near the Franck–Condon region, and their energies are close (<2 kcal/mol) to the energy of the Franck–Condon point. An especially interesting case is the V-shaped structure shown in Figure 5, which exhibits a face-to-face orientation of the π -conjugated systems on the STIL and DMAS. Consequently, the HOMO–LUMO spatial overlap is maximized in this geometry, and therefore, it represents a bright S_1 CT electronic state with an emission wavelength of 506 nm (Table 4). In addition, the state has a large molecular dipole because of its strong CT character. Such CT emission wavelength and expected strong solvent polarity dependence are in excellent agreement with experimental observations.^{8,10,16} The results indicate that once

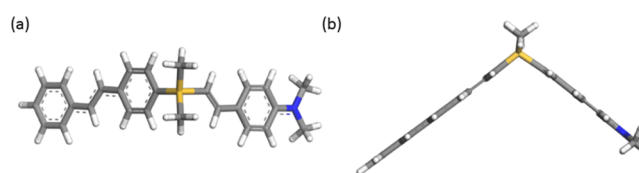


Figure 5. Structure of the V-shape DA-Me-VS conformer. (a) Top view and (b) side view.

Table 4. Calculated Excited-State Properties of DA-Me-VS (TDDFT/B3LYP/6-31+G(d))

state	λ (nm)	f	major configuration(s) ^a	μ^b	character
S_1	506	0.11	H → L (100%)	36.7	CT _{D→A}
S_2	372	1.32	H − 1 → L (93%)	4.1	LE _A
S_3	324	0.48	H → L + 1 (85%)	9.9	LE _D

^aPopulation > 10%. ^bUnit: debye.

the CT state is populated following the nonadiabatic transition from the S_2 excited state, the conformational dynamics along the D5 and D6 rotation could easily bring the CT state into an emissive structure, hence the CT band in the dual emission of the DA dimer and copolymer systems in polar solvents. Note that in our calculations the TICT state remains non-emissive regardless of the conformational structures; the V-shaped emissive state corresponds to a delocalized DMAS-to-STIL CT state.

4. CONCLUSIONS

We apply TDDFT to investigate excited-state properties of a dimethylsilylene-spaced dimethylaminostyrene–stilbene DA dimer system (DA-Me) in order to elucidate the complex energy transfer and electron transfer dynamics in oligomers and copolymers of similar DA systems. We demonstrate that the vertical S_3 , S_2 , and S_1 excited states of DA-Me are local excitation on the aminostyrene, local excitation on the stilbene, and CT state, respectively. In addition, we also discover an energy minimum on the S_1 PES with C–N bond of the amino group twisted at about 90° , which corresponds to an S_1 TICT state. To fully elucidate the excited-state chemical dynamics that would significantly affect the energy and charge transfer processes in DA-Me, we apply potential energy scan along

important bond rotation coordinates to map out the potential energy curves for the excited states of **DA-Me**. In particular, we found that the C–N bond torsional angle significantly affects the excited-state characteristics of **DA-Me**, and a conical intersection between the S_2 stilbene local excitation and the S_1 CT/TICT state is revealed at a C–N bond torsional angle of $\sim 60^\circ$. Through this conical intersection, the optically allowed photoexcitation into the S_2 state can generate both the delocalized CT state and the localized TICT state, depending on the energetics of the PES. Moreover, conformational changes using rotations of the two chromophores reveal an emissive dimer with a V-shape conformational structure despite the zero oscillator strength of the S_1 excited states in the CT minimum energy geometries. As a result, relaxation into the S_1 CT state followed by conformational changes could lead to CT emission from the S_1 state.

We summarize our results in the energy-level diagram presented in Figure 6, and the data finally provide a clear

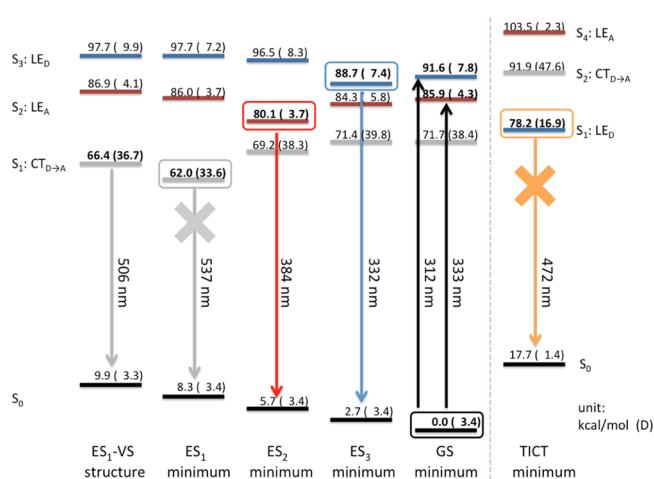


Figure 6. Energy-level diagrams for various structures of the **DA-Me-Sa⁻** system. For each state, the relative energy in the unit of kcal/mol is labeled, and the magnitude of transition dipole with respect to the GS in the unit of debye is given in parentheses.

explanation of the complex photophysics and solvent-polarity dependence observed in **DA-Me**. In nonpolar solvents, such as hexane and cyclohexane, experiments show that **DA-Me** exhibits a single LE emission centered around 360–370 nm,^{8,10} which is in good agreement with the TDDFT-predicted S_2 emission of the stilbene $\pi\pi^*$ excited state at 384 nm. Time-resolved transient absorption study of **DA-Me** in cyclohexane reveals rapid ~ 1.2 ps energy transfer,¹⁶ which is consistent with the expected rapid $S_3 \rightarrow S_2$ nonadiabatic transition in our results. Previously, the lack of CT emission band and CT dynamics for **DA-Me** in nonpolar solvents was puzzling. On the basis of the exploration of the excited-state PES, we propose that the conical intersection between S_1 and S_2 along the C–N bond rotation dominates the electron transfer dynamics in **DA-Me**, and the energy barrier between the Franck–Condon structure and the conical intersection controls the efficiency of the electron transfer. Our calculations indicate that the energy barrier is relatively high in nonpolar solvents (~ 6 kcal/mol), which explains why charge transfer is not observed for **DA-Me** in nonpolar solvents.

In polar solvents such as tetrahydrofuran (THF), **DA-Me** demonstrates distinctive photophysical properties. Dual

emission with clear CT band is observed, and rapid charge transfer from dimethylaminostyrene to stilbene also occurs. Our calculations indicate that the stabilization of CT and TICT states as solvent polarity increases likely contributes to the lowering of the energy barrier for the Franck–Condon excitation of S_2 to reach the conical intersection on the S_2 PES, because the electronic state at the crossing point is a mixture of the LE and CT states, whereas the S_2 state near the Franck–Condon region is an LE state. Therefore, increased solvent polarity should facilitate efficient electron transfer and population of the delocalized CT state in polar solvents. It is also interesting to note that the molecular dipole moment of the emissive V-shaped S_1 state is slightly larger than that of the S_1 CT minimum state (Figure 6), indicating that the V-shaped structure would be more easily accessible in polar solvents. The emission wavelength of the V-shaped CT state is predicted to be 506 nm, which is in agreement with the position of the observed CT band (~ 510 nm in THF).

Experiments further showed that in solvents with very strong polarity, such as MeOH and acetonitrile, the CT emission disappears, whereas the electron transfer process remains efficient. Our results cannot address this issue directly because we have not considered solvation effects in our calculations. Nevertheless, based on the PES reported in Figures 3 and 6, we suspect that the change in the energy barrier and the location of the conical intersection because of different levels of stabilization in the CT state compared to the TICT state could be responsible for the disappearance of the CT band in strongly polar solvents. This issue is complicated and requires further calculations to clarify. Calculations of the excited-state properties of **DA-Me** with the inclusion of solvation effects are currently works in progress and will be reported in a separated paper.

We emphasize the crucial roles of nonadiabatic dynamics and the C–N bond rotation in the photophysical properties of the **DA-Me** system, and we suggest that such mechanisms also play important roles in the photophysical properties of more extended alternating oligomer and copolymer systems. In particular, the influence of the degree of polymerization and the Thorpe–Ingold effect induced by replacing the two methyl groups on the silylene with two more bulky isopropyl groups has been shown to drastically change the polymer folding and photophysical properties of the silylene-spaced aminostyrene–stilbene copolymers.^{8,10} It would be interesting to explore the role of C–N bond rotation in these more sterically hindered systems. More importantly, the identifications of the conical intersection and energy barrier along the C–N bond rotation provide a novel synthetic route to the control of emissive properties and electron transfer dynamics in DA systems with amino substituents, which might be useful in the design of functional organic optoelectronic materials and artificial photosynthetic systems.

■ ASSOCIATED CONTENT

Supporting Information

The Supporting Information is available free of charge on the ACS Publications website at DOI: 10.1021/acs.jpca.9b00856.

Additional computational results and figures (PDF)

■ AUTHOR INFORMATION

Corresponding Author

*E-mail: yuanchung@ntu.edu.tw.

ORCID 

Yuan-Chung Cheng: 0000-0003-0125-4267

Author Contributions

The paper was written through contributions of all authors. All authors have given approval to the final version of the paper.

Notes

The authors declare no competing financial interest.

ACKNOWLEDGMENTS

Y.-C.C. thanks the Ministry of Science and Technology, Taiwan (grant no. MOST 107-2113-M-002-001), National Taiwan University (grant no. 108L893205), for financial support. We are grateful to Computer and Information Networking Center, National Taiwan University, for the support of high-performance computing facilities. We are grateful to the National Center for High-Performance Computing for computer time and facilities.

ABBREVIATIONS

DFT, density functional theory; TDDFT, time-dependent density functional theory; STIL, stilbene; DMAS, dimethylaminostyrene; PES, potential energy surface

REFERENCES

- (1) Turro, N. J.; Ramamurthy, V.; Scaiano, J. C. *Principles of Molecular Photochemistry: An Introduction*; University Science Books: Sausalito, California, 2009.
- (2) Brédas, J.-L.; Beljonne, D.; Coropceanu, V.; Cornil, J. Charge-Transfer and Energy-Transfer Processes in Pi-Conjugated Oligomers and Polymers: a Molecular Picture. *Chem. Rev.* **2004**, *104*, 4971–5003.
- (3) Brouwer, H. J.; Krasnikov, V. V.; Hilberer, A.; Hadziioannou, G. Blue Superradiance From Neat Semiconducting Alternating Copolymer Films. *Adv. Mater.* **1996**, *8*, 935–937.
- (4) Jung, S.-H.; Kim, H. K.; Kim, S.-H.; Kim, Y. H.; Jeoung, S. C.; Kim, D. Palladium-Catalyzed Direct Synthesis, Photophysical Properties, and Tunable Electroluminescence of Novel Silicon-Based Alternating Copolymers. *Macromolecules* **2000**, *33*, 9277–9288.
- (5) Cheng, Y.-J.; Hwu, T.-Y.; Hsu, J.-H.; Luh, T.-Y. Intrachain Energy Transfer in Silylene-Spaced Alternating Donor-Acceptor Divinylarene Copolymers. *Chem. Commun.* **2002**, *118*, 1978–1979.
- (6) Liu, K.-L.; Lee, S.-J.; Chen, I.-C.; Hsu, C.-P.; Chen, C.-H.; Luh, T.-Y. Ultrafast Energy Transfer in Divinylbiphenyl and Divinylstilbene Copolymers Bridged by Silylene. *J. Phys. Chem. C* **2013**, *117*, 64–70.
- (7) Wang, H.-W.; Cheng, Y.-J.; Chen, C.-H.; Lim, T.-S.; Fann, W.; Lin, C.-L.; Chang, Y.-P.; Lin, K.-C.; Luh, T.-Y. Photoinduced Electron Transfer in Silylene-Spaced Copolymers Having Alternating Donor-Acceptor Chromophores. *Macromolecules* **2007**, *40*, 2666–2671.
- (8) Liao, W.-C.; Chen, W.-H.; Chen, C.-H.; Lim, T.-S.; Luh, T.-Y. Photoinduced Electron Transfer as a Probe for the Folding Behavior of Dimethylsilylene-Spaced Alternating Donor-Acceptor Oligomers and Polymers. *Macromolecules* **2013**, *46*, 1305–1311.
- (9) Yeh, M.-Y.; Luh, T.-Y. Thorpe-Ingold Effect on the Helicity of Chiral Alternating Silylene-Divinylarene Copolymers. *Chem.—Asian J.* **2008**, *3*, 1620–1624.
- (10) Chen, C.-H.; Huang, Y.-C.; Liao, W.-C.; Lim, T.-S.; Liu, K.-L.; Chen, I.-C.; Luh, T.-Y. Controlling Conformations in Alternating Dialkylsilylene-Spaced Donor-Acceptor Copolymers by a Cooperative Thorpe-Ingold Effect and Polymer Folding. *Chem.—Eur. J.* **2012**, *18*, 334–346.
- (11) Chen, C.-H.; Chen, W.-H.; Liu, Y.-H.; Lim, T.-S.; Luh, T.-Y. Folding of Alternating Dialkylsilylene-Spaced Donor-Acceptor Copolymers: the Oligomer Approach. *Chem.—Eur. J.* **2012**, *18*, 347–354.
- (12) van Walree, C. A.; Roest, M. R.; Schuddeboom, W.; Jennekens, L. W.; Verhoeven, J. W.; Warman, J. M.; Kooijman, H.; Spek, A. L. Comparison Between SiMe(2) and CMe(2) Spacers as Sigma-Bridges for Photoinduced Charge Transfer. *J. Am. Chem. Soc.* **1996**, *118*, 8395–8407.
- (13) Wang, H.-W.; Yeh, M.-Y.; Chen, C.-H.; Lim, T.-S.; Fann, W.; Luh, T.-Y. Coupling of FRET and Photoinduced Electron Transfer in Regioregular Silylene-Spaced Energy Donor-Acceptor-Electron Donor Copolymers. *Macromolecules* **2008**, *41*, 2762–2770.
- (14) Liu, K.-L.; Lee, S.-J.; Chen, I.-C.; Hsu, C.-P.; Yeh, M.-Y.; Luh, T.-Y. Ultrafast Energy Transfer in a Regioregular Silylene-Spaced Copolymer. *J. Phys. Chem. C* **2010**, *114*, 13909–13916.
- (15) Liu, K.-L.; Lee, S.-J.; Chen, I.-C.; Hsu, C.-P.; Yeh, M.-Y.; Luh, T.-Y. Excited-State Dynamics of [(1,1'-Biphenyl)-4,4'-diylidene-2,1-ethenediyl]bis(dimethylsilylene). *J. Phys. Chem. A* **2009**, *113*, 1218–1224.
- (16) Yao, H.-H.; Chung, M.-R.; Huang, C.; Lin, S. M.-H.; Chen, C.-H.; Luh, T.-Y.; Chen, I.-C. Charge and Energy Transfer Dynamics in Dimethylsilylene-Spaced Aminostyrene Stilbene Monomer Using Time-Resolved Techniques. *J. Phys. Chem. A* **2017**, *121*, 7079–7088.
- (17) Shuai, Z.; Wang, D.; Peng, Q.; Geng, H. Computational Evaluation of Optoelectronic Properties for Organic/Carbon Materials. *Acc. Chem. Res.* **2014**, *47*, 3301–3309.
- (18) Soler, M. A.; Nelson, T.; Roitberg, A. E.; Tretiak, S.; Fernandez-Alberti, S. Signature of Nonadiabatic Coupling in Excited-State Vibrational Modes. *J. Phys. Chem. A* **2014**, *118*, 10372–10379.
- (19) Nelson, T.; Fernandez-Alberti, S.; Roitberg, A. E.; Tretiak, S. Nonadiabatic Excited-State Molecular Dynamics: Modeling Photo-physics in Organic Conjugated Materials. *Acc. Chem. Res.* **2014**, *47*, 1155–1164.
- (20) Fan, D.; Yi, Y.; Li, Z.; Liu, W.; Peng, Q.; Shuai, Z. Solvent Effects on the Optical Spectra and Excited-State Decay of Triphenylamine-Thiadiazole with Hybridized Local Excitation and Intramolecular Charge Transfer. *J. Phys. Chem. A* **2015**, *119*, 5233–5240.
- (21) Wang, J.; Huang, J.; Du, L.; Lan, Z. Photoinduced Ultrafast Intramolecular Excited-State Energy Transfer in the Silylene-Bridged Biphenyl and Stilbene (SBS) System: a Nonadiabatic Dynamics Point of View. *J. Phys. Chem. A* **2015**, *119*, 6937–6948.
- (22) Lambert, C.; Koch, F.; Völker, S. F.; Schmiedel, A.; Holzapfel, M.; Humeniuk, A.; Röhr, M. I. S.; Mitric, R.; Brixner, T. Energy Transfer Between Squaraine Polymer Sections: From Helix to Zigzag and All the Way Back. *J. Am. Chem. Soc.* **2015**, *137*, 7851–7861.
- (23) Alfonso Hernandez, L.; Nelson, T.; Tretiak, S.; Fernandez-Alberti, S. Photoexcited Energy Transfer in a Weakly Coupled Dimer. *J. Phys. Chem. B* **2015**, *119*, 7242–7252.
- (24) Frisch, M. J.; Trucks, G. W.; Schlegel, H. B.; Scuseria, G. E.; Robb, M. A.; Cheeseman, J. R.; Scalmani, G.; Barone, V.; Mennucci, B.; Petersson, G. A.; et al. *Gaussian 09*, Revision D.01; Gaussian, Inc.: Wallingford CT, 2009.
- (25) Stephens, P. J.; Devlin, F. J.; Chabalowski, C. F.; Frisch, M. J. Ab Initio Calculation of Vibrational Absorption and Circular Dichroism Spectra Using Density Functional Force Fields. *J. Phys. Chem.* **1994**, *98*, 11623–11627.
- (26) Grimme, S.; Antony, J.; Ehrlich, S.; Krieg, H. A Consistent and Accurate Ab Initio Parametrization of Density Functional Dispersion Correction (DFT-D) for the 94 Elements H-Pu. *J. Chem. Phys.* **2010**, *132*, 154104.
- (27) Zhao, Y.; Truhlar, D. G. The M06 Suite of Density Functionals for Main Group Thermochemistry, Thermochemical Kinetics, Noncovalent Interactions, Excited States, and Transition Elements: Two New Functionals and Systematic Testing of Four M06-Class Functionals and 12 Other Functionals. *Theor. Chem. Acc.* **2008**, *120*, 215–241.
- (28) Halgren, T. A.; Lipscomb, W. N. Synchronous-Transit Method for Determining Reaction Pathways and Locating Molecular Transition-States. *Chem. Phys. Lett.* **1977**, *49*, 225–232.
- (29) Cogan, S.; Zilberg, S.; Haas, Y. The Electronic Origin of the Dual Fluorescence in Donor-Acceptor Substituted Benzene Derivatives. *J. Am. Chem. Soc.* **2006**, *128*, 3335–3345.

(30) Chiba, M.; Tsuneda, T.; Hirao, K. Long-range corrected time-dependent density functional study on fluorescence of 4,4'-dimethylaminobenzonitrile. *J. Chem. Phys.* **2007**, *126*, 034504.

(31) Gustavsson, T.; Coto, P. B.; Serrano-Andrés, L.; Fujiwara, T.; Lim, E. C. Do Fluorescence and Transient Absorption Probe the Same Intramolecular Charge Transfer State of 4-(Dimethylamino)-Benzonitrile? *J. Chem. Phys.* **2009**, *131*, 031101.

(32) Haberhauer, G. Planarized and Twisted Intramolecular Charge Transfer: a Concept for Fluorophores Showing Two Independent Rotations in Excited State. *Chem.—Eur. J.* **2017**, *23*, 9288–9296.